

# The Ground State Structures and Magnetic Properties of $Zr_nNi$ ( $n = 1-9$ ) Clusters from First Principles Calculation

Y.L. ZHANG<sup>a,b,\*</sup>, Z.Q. ZHU<sup>a</sup>, X.D. ZHOU<sup>c</sup>, J. YANG<sup>a</sup> AND Y. ZHU<sup>a</sup>

<sup>a</sup>School of Physics and Telecommunication Engineering, Zhoukou Normal University, Zhoukou 466001, PRC

<sup>b</sup>Department of Physics, Zhejiang University, Hangzhou 310027, PRC

<sup>c</sup>School of Mechanical and Electrical Engineering, Zhoukou Normal University, Zhoukou 466001, PRC

(Received August 23, 2016; revised version April 10, 2017; in final form May 3, 2017)

The ground state structures and magnetic properties of  $Zr_nNi$  ( $n = 1-9$ ) clusters are studied by using first principles calculation. Firstly, we find the ground state configurations of  $Zr_nNi$  ( $n = 1-9$ ) clusters. Secondly, the magic clusters ( $Zr_2Ni$  and  $Zr_7Ni$ ) of  $Zr_nNi$  clusters are found by the comparisons of average binding energies, the second-order energy difference and energy gaps between the highest occupied orbital and the lowest unoccupied orbital of the ground state of  $Zr_nNi$  clusters. Thirdly, the calculated results show that magnetic moment of  $Zr_nNi$  ( $n = 1-2$ ) clusters is  $4 \mu_B$ ; however, the magnetic moment of  $Zr_nNi$  clusters is about  $2 \mu_B$  for  $n = 3-9$  (exception for  $n = 7$ ). Finally, it is found that the magnetic moment of  $Zr_nNi$  cluster mainly comes from Zr atom and Ni atom is the electron acceptor from the Mulliken population analysis.

DOI: [10.12693/APhysPolA.131.1507](https://doi.org/10.12693/APhysPolA.131.1507)

PACS/topics: first-principles calculations,  $Zr_nNi$  clusters, the geometric structure of balance, stability and magnetic properties

## 1. Introduction

Atomic cluster shows new physical phenomena due to quantum size effect, macroscopic quantum tunneling effect and surface effect, which make it fit for the design and synthesis of new materials, thus, atom cluster attract the attention of many theoretical and experimental workers in recent 30 years [1–14].

Transition metal cluster shows new properties in the geometry, electronic structure and magnetic characteristics, so it becomes the focus of attention of people [15–20]. Zirconium (Zr) is used as the cladding of fuel in the nuclear industry due to its less absorption of neutron. Zr is also used for refining alloy instead of steel because its strong corrosion resistance to common acid, alkali and salt, besides, also has been used in surgery and chemical industry, all of these are the reasons why people pay attention to  $Zr_n$  and corresponding mixed clusters [21–25]. Wang et al. find that the magic numbers of stabilities are  $n = 2, 5,$  and  $7$  and the atomic averaged magnetic moments of the  $Zr_n$  ( $n \neq 2$ ) display an odd-even oscillation features, the tetrahedron  $CsZr_4$  structure has the biggest atomic averaged magnetic moment of  $1.5 \mu_B/\text{atom}$  [22]; Zhao et al. find that the relative stabilities of  $Zr_5Fe$ ,  $Zr_7Fe$  and  $Zr_{12}Fe$  are stronger than that of other sized clusters and they are all magnetic clusters for  $Zr_nFe$  ( $n = 2-13$ ) [24]; Ren et al. find that the relative stabilities of  $Zr_4Co$ ,  $Zr_7Co$ ,  $Zr_9Co$ , and  $Zr_{12}Co$  are stronger than other sized clusters, and the magnetic moment of  $Zr_nCo$  clusters mainly comes from the localized  $d$  electron [25]. It is found that the magnetic moment of the smaller clusters  $Zr_2Fe$ ,  $Zr_4Fe$ ,  $ZrCo$ ,

and  $Zr_2Co$  mainly came from Zr atoms based on the analysis of the data in Refs. [24, 25]. As transition element, nickel (Ni) has lots of physical and chemical properties, Ni can be used not only as permanent magnetic material but also as an important alloy element. Not only pure Ni clusters are the focus of attention [9, 26], Ni–Nb alloy has been used in superconducting magnet, the systems show many peculiar properties in the structure and electronic properties when Ni is doped in semiconductor silicon, germanium and bivalent alkali metal clusters [27–29]. Ni and Zr alloy has superconducting property [30], what is more important is that it has many advantages compared with other alloy glass, such as positive hall coefficient [31], quantum interference effect [32], big induction conductivity of anisotropy [33], besides, it can exist in large doping concentration scope, therefore the Zr–Ni alloy attracts people’s attention [34–36]. However, by now the research on geometrical structure and other properties of  $Zr_nNi$  clusters in experiment and theory is rare.

The geometric structures, average binding energies, the second-order differences of energy, the energy gaps between the highest occupied molecular orbital (HOMO) and the lowest unoccupied molecular orbital (LUMO), the magnetic properties of  $Zr_nNi$  clusters and the magnetic moment of Zr (Ni) atom are studied in this paper, the results are useful for related research.

## 2. Computational method

In order to find the ground state structures of  $Zr_nNi$  clusters, a large number of possible initial structures for each size of the clusters are considered in this paper. Three ways are adopted to construct the initial configurations of  $Zr_nNi$ . The first method to get the initial configurations of  $Zr_nNi$  is by using Ni to replace M atom of the equilibrium configurations of  $Zr_nM$  ( $M = Fe, Co$ )

\*corresponding author; e-mail: [zhangyunli0558@163.com](mailto:zhangyunli0558@163.com)

clusters [24, 25]; in the second method a variety of possible configurations are built by Ni atom blocking (or gap filling) based on all the balance configurations of  $Zr_n$  clusters [21–23] or by possible replacement of Zr atom in  $Zr_{n+1}$  clusters to get the initial configurations of  $Zr_nNi$  clusters. The third way to look for the initial configurations of  $Zr_nNi$  clusters is taking the equilibrium configuration of titanium [37, 38] and cadmium [39] clusters for reference.

The calculations in full geometry optimization are performed using spin-polarized density functional method in Dmol3 simulation package (ver. 3.2) [40] and the calculations in the electronic structure are performed using effective nuclear potential and a double numerical basis including a  $d$ -polarization function, and the exchange and correlation potential is GGA-PW91 method [41]. The convergence criteria of self consistent field is  $10^{-5}$  Ha, the convergence criteria of force is 0.04 Ha/nm, displacement convergence criteria is 0.0005 nm in the process of geometric optimization and the convergence standard energy is  $10^{-5}$  Ha.  $Zr_nNi$  clusters who have even number of electrons are studied starting from spin singlet, the method of spin non-restriction is used in the calculation, and all possible spin multiplicity are optimized. In order to verify the reliability of the method used in this article, firstly, dimer  $Zr_2$ , whose experimental data can be contrasted, are calculated. The result show that the Zr–Zr bond length (0.2324 nm) is consistent with the results of calculation well [22, 23, 42, 43], which means that the method chosen in this paper is reasonable.

### 3. Results and discussion

#### 3.1. Geometrical structures of $Zr_nNi$ clusters

The equilibrium structures of  $Zr_nNi$  clusters are shown in Fig. 1, the dark balls are on behalf of Ni atoms and the light color balls are on behalf of Zr atoms. The balance structures of clusters are marked as  $na$ ,  $nb$ ,  $nc$ , and so on for any specific size and their energies change from low to high, where  $na$  stand for ground state of  $Zr_nNi$  cluster. Physical quantities such as spin multiplicities, symmetry and energy difference of equilibrium structure ( $nb$ ,  $nc$ , and so on) and ground state ( $na$ ) on  $Zr_nNi$  are listed in Fig. 1. In fact, the spin multiplicities are fully considered for all configurations. The energies of all spin states are considered and calculated for all the balance configurations. But in the following only the lowest energy states of steady state are talked.

The symmetric configuration of  $ZrNi$  ground state is 1a, of which spin state is quintuplet, Zr–Ni bond length is 0.2446 nm. For  $Zr_2Ni$  clusters, its ground state is an isosceles triangle structure as 2a ( $C_{2v}$ ), whose apex angle is  $65.23^\circ$ , Zr–Ni bond length is 0.2406 nm, Zr–Zr bond length is 0.2593 nm and spin state is also quintuplet, which shows Zr–Zr bond length is longer than that of Ni–Zr in  $Zr_2Ni$  cluster agreeing with the result in Ref. [44]; another kind of configuration is linear type with Ni in the center of symmetry, its energy is 1.940 eV higher than the ground state energy. The ground state (3a) of

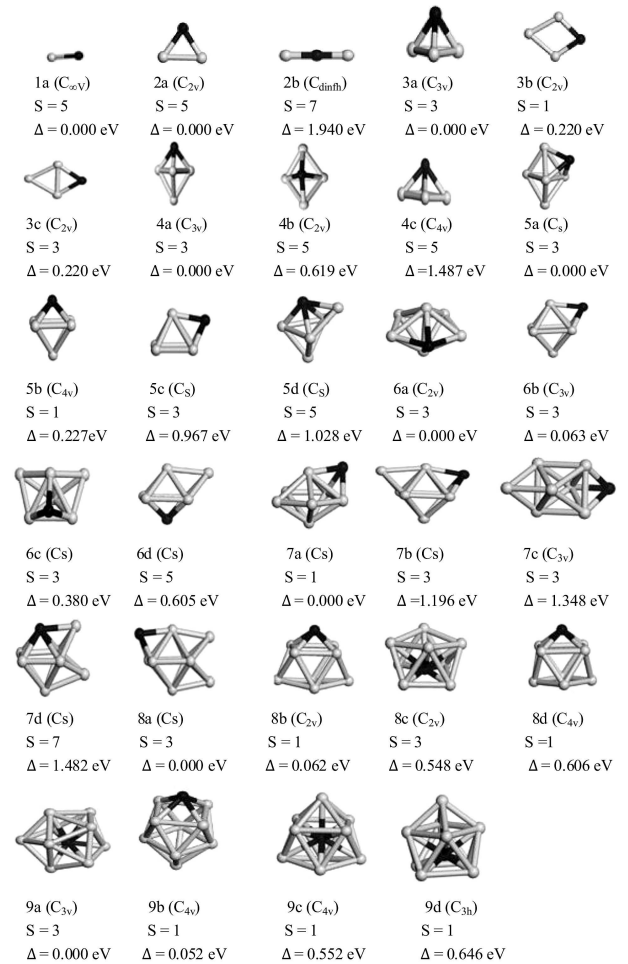


Fig. 1. The equilibrium structures, symmetries, multiplicity  $S$  and energy difference  $\Delta E$  between equilibrium state and base state of  $Zr_nNi$  clusters. (1) The dark balls are on behalf of Ni atoms and the light color balls are on behalf of Zr atoms. (2) The equilibrium structures of clusters are marked as  $na$ ,  $nb$ ,  $nc$ , and so on for any specific size. (3) Spin multiplicity, symmetry and energy difference of equilibrium structure ( $nb$ ,  $nc$ , and so on) and ground state  $na$  of  $Zr_nNi$  are listed in figure.

$Zr_3Ni$  is spin triplet with  $C_{3v}$  tetrahedron symmetry, other structures of  $Zr_3Ni$  are of  $C_{2v}$  symmetry as shown, 3b and 3c, they are spin singlet and spin triplet respectively, both their energy is 0.220 eV higher than that of  $Zr_3Ni$  ground state. The balance geometric structures of  $Zr_4Ni$  are obtained as shown, 4a ( $C_{3v}$ ), 4b ( $C_{2v}$ ), 4c ( $C_{4v}$ ) in Fig. 1. They are double cone, twin double cone and right square pyramid, the energies of 4b ( $C_{2v}$ ), 4c ( $C_{4v}$ ) are 0.619 and 1.487 eV higher than that of 4a ( $C_{3v}$ ), respectively. 4a ( $C_{3v}$ ) is the ground state of  $Zr_4Ni$  and its spin is triplet. The ground state (5a) of  $Zr_5Ni$  is triangular bipyramid and whose spin state is triplet, the geometric configuration ( $C_s$ ) of which is gained by blocking a Ni atom to the ground state  $Zr_5$  [23], and the rest of the balance structures of  $Zr_5Ni$  are also shown as 5b ( $C_{4v}$ ), 5c ( $C_s$ ) and 5d ( $C_s$ ) in Fig. 1, and their energies are 0.227, 0.976, and 1.028 eV higher than the energy of the ground

state. It can be seen from Fig. 1 that the pentagon double cone structure  $6a$  ( $C_s$ ) is the ground state and its spin state is triplet, the rest of the balance structure as shown  $6b$  ( $C_{3v}$ ),  $6c$  ( $C_s$ ) and  $6d$  ( $C_s$ ) and their energies are 0.063, 0.380, and 0.605 eV higher than that of its ground state, respectively. The ground state of  $Zr_7Ni$  is spin singlet with geometric configuration as  $7a$  ( $C_s$ ), which is obtained by blocking a Ni atom to a little distortion double cone, and the rest of the three isomers are shown as  $7b$  ( $C_s$ ),  $7c$  ( $C_{3v}$ ) and  $7d$  ( $C_s$ ), their energies are 1.196, 1.348, and 1.482 eV higher than the energy of its ground state. It is found that  $Zr_7Ni$  ground state is the most stable of  $Zr_nNi$  clusters through the following analysis, which is similar to the results of literatures [24, 25], where  $Zr_7Fe$  and  $Zr_7Co$  are the stable states of  $Zr_nFe$  and  $Zr_nCo$ . The ground state structure of  $Zr_8Ni$  clusters is shown as  $8a$  ( $C_s$ ), whose spin is triplet, which is not the same as the  $Zr_8Fe$  and  $Zr_8Co$  structures in literature [24, 25], the balance of the other structure as shown  $8b$  ( $C_{2v}$ ),  $8c$  ( $C_{2v}$ ),  $8d$  ( $C_{4v}$ ), their energies are 0.062, 0.548, and 0.606 eV higher than that of the ground state. The structure of the ground state on  $Zr_9Ni$  is shown as  $9a$  ( $C_{3v}$ ), whose spin is triplet, the other balance structures for  $Zr_9Ni$  are shown as  $9b$  ( $C_{4v}$ ),  $9c$  ( $D_{3h}$ ),  $9d$  ( $C_{4v}$ ), their energy is 0.052, 0.552, and 0.646 eV higher than that of the ground state, respectively.

### 3.2. The relative stability of $Zr_nNi$ clusters

Average binding energy  $E_b$ , the second-order difference energy  $\Delta_2E$  and energy gap  $E_{gap}$  (energy difference between HOMO and LUMO) of the ground state have been calculated and the results have been listed in Table I.

TABLE I

Atomic averaged binding energy  $E_b$ , the second-order difference energies  $\Delta_2E_n$ , and energy gap  $E_{gap}$  between HOMO (the highest occupied orbital) and LUMO (the lowest unoccupied orbital) for the ground state  $Zr_nNi$  ( $n = 2-9$ ) clusters.

| Cluster  | $E_b$ [eV] | $\Delta_2E_n$ [eV] | $E_{gap}$ [eV] |
|----------|------------|--------------------|----------------|
| $ZrNi$   | 1.420      |                    | 0.008          |
| $Zr_2Ni$ | 2.960      | 0.195              | 0.320          |
| $Zr_3Ni$ | 3.423      | -0.585             | 0.220          |
| $Zr_4Ni$ | 3.813      | 0.171              | 0.115          |
| $Zr_5Ni$ | 4.044      | 0.105              | 0.163          |
| $Zr_6Ni$ | 4.195      | -0.504             | 0.129          |
| $Zr_7Ni$ | 4.371      | 0.937              | 0.443          |
| $Zr_8Ni$ | 4.403      | -0.467             | 0.208          |
| $Zr_9Ni$ | 4.476      |                    | 0.338          |

In order to describe their properties, the results have been shown in Figs. 2–4, respectively. The average binding energy and the definition of second-order difference energies are as follows:

$$E_b(n) = \frac{(nE_t(Zr) + E_t(Ni) - E_t(Zr_nNi))}{n+1}, \quad (1)$$

$$\Delta_2E(n) = E_t(Zr_{n+1}Ni) + E_t(Zr_{n-1}Ni) - 2E_t(Zr_nNi). \quad (2)$$

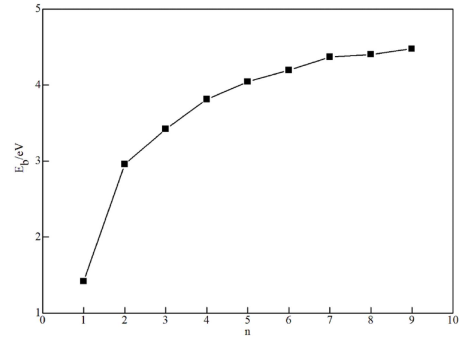


Fig. 2. Size dependence of average binding energy  $E_b$  of the ground state  $Zr_nNi$  clusters.

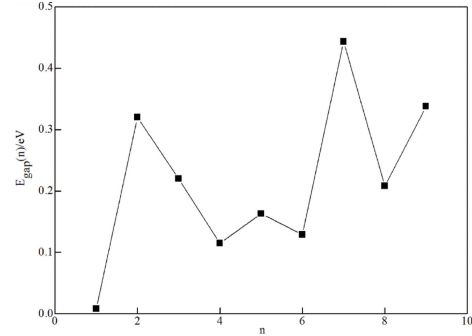


Fig. 3. Size dependence of energy gap  $E_{gap}$  of the ground state  $Zr_nNi$  clusters.

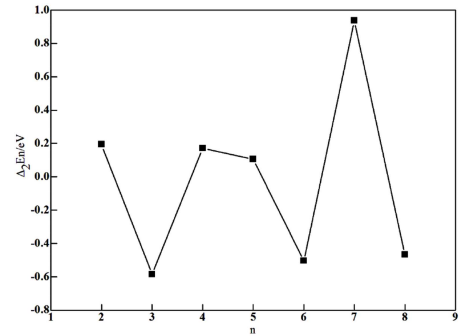


Fig. 4. Size dependence of the second-order difference energies  $\Delta_2E_n$  of the ground state  $Zr_nNi$  clusters.

Here  $E_t(Zr)$ ,  $E_t(Ni)$ ,  $E_t(Zr_{n-1}Ni)$ ,  $E_t(Zr_nNi)$ , and  $E_t(Zr_{n+1}Ni)$  represent energies of the corresponding atoms and clusters, respectively. Figure 2 shows that the average binding energy increases with the size of cluster becoming large. The average binding energy of cluster grows rapidly for  $n$  changing from 1 to 2 and 6 to 7, however the change of the binding energy is slower for  $n$  changing from 2 to 5 and 7 to 9. There is a local maximum for  $n = 2, 7$ , which means that these clusters are more stable than their neighboring clusters. As we know the size of the  $E_{gap}$  reflects the ability of the electronic transition from HOMO to LUMO, to some extent,  $E_{gap}$  represents the ability to participate in chemical reactions. Figure 3 shows the change rule of  $E_{gap}$  with its size, from which it can be seen that local maximum of  $E_{gap}$  appears at  $n = 2, 5, 7$ , which further indicates

the stability of the corresponding clusters are higher than other clusters. In the field of clusters physics, the greater the second-order energy difference the more stable of clusters. Figure 4 shows the change law of  $\Delta_2E$  with its size. It can be seen that when  $n = 2, 7$ ,  $\Delta_2E$  appears local maximum, which means that these clusters are more stable being coincident with the results of  $E_{gap}$ . Both the energy gap and second-order energy difference of  $Zr_7Ni$  are the biggest in all clusters, and its value is far greater than other clusters, suggesting that the singlet state of  $Zr_7Ni$  is the most stable of all  $Zr_nNi$  ( $n = 1-9$ ), the exceptional stability to the singlet state of  $Zr_7Ni$  can be explained by the jellium model of metal clusters [45]. Zr has 4 valence electrons whereas Ni has 10. In  $Zr_7Ni$ , there are  $7 \times 4 + 10 = 38$  valence electrons. 2 of them can be considered to complete Ni 3d orbital and the remaining 36 electrons may be considered for the construction of a closed super atomic shell. It is not difficult to draw from Figs. 2-4 that  $Zr_2Ni$  and  $Zr_7Ni$  are magic number of  $Zr_nNi$ , they can be gotten by capping a Ni atom to the stable structures of  $Zr_2$  and  $Zr_7$  [23], respectively.

### 3.3. Magnetic property of $Zr_nNi$ clusters

The occupied number of electrons orbital can be gotten by the analysis of the Mulliken population, and the average magnetic moment has been obtained by calculating the difference of electron occupation number between spin up state and spin down state. The total magnetic moment of the clusters, magnetic moment of Zr and Ni atoms of the ground state are presented in Table II. It can be seen from Table II that the magnetic moment of clusters system mainly comes from the contribution of Zr atom, and the magnetic moment of clusters can be divided into two parts:  $Zr_nNi$  clusters almost have stable magnetic moment  $4 \mu_B$  for  $n = 1-2$ , however the magnetic moment of  $Zr_nNi$  is basically stable in  $2 \mu_B$  for  $n = 2-9$  (except for  $n = 7$ ) clusters, which is very similar to  $Ge_nFe$  clusters [46]. It also can be seen that Ni atom gets charge from Zr atom by the Mulliken population analysis.

TABLE II

Total magnetic moment of  $Zr_nNi$ , average atomic magnetic moment of Zr atom, atomic magnetic moment of Ni atom and charge  $C_{Ni}$  of Ni atom on the ground state  $Zr_nNi$  ( $n = 2-9$ ) clusters.

| Cluster  | Magnetic moment [ $\mu_B$ ] |       |        | Charge [ $e$ ] |
|----------|-----------------------------|-------|--------|----------------|
|          | $Zr_nNi$                    | Zr    | Ni     | Ni             |
| $ZrNi$   | 4.0                         | 2.983 | 1.017  | -0.129         |
| $Zr_2Ni$ | 4.0                         | 3.734 | 0.266  | -0.124         |
| $Zr_3Ni$ | 1.999                       | 1.638 | 0.361  | -0.089         |
| $Zr_4Ni$ | 2.0                         | 2.003 | -0.003 | -0.039         |
| $Zr_5Ni$ | 1.998                       | 1.754 | 0.246  | -0.129         |
| $Zr_6Ni$ | 1.968                       | 1.447 | 0.521  | -0.088         |
| $Zr_7Ni$ | 0                           | 0     | 0      | -0.210         |
| $Zr_8Ni$ | 1.999                       | 1.764 | 0.235  | -0.162         |
| $Zr_9Ni$ | 2.261                       | 2.155 | 0.106  | -0.247         |

### 3.4. The electronic properties of a typical cluster $Zr_2Ni$

The total and partial density of states of Zr and Ni atom for both up and down spins on the typical cluster  $Zr_nNi$  ( $n = 2$ ) are shown in Fig. 5 in order to verify our calculated result that the magnetic moment of  $Zr_nNi$  cluster mainly coming from Zr atom is reasonable, from which it can be seen that the total density of states of Ni and Zr atom for both up and down spins are not symmetrical and the magnetic moment of  $Zr_2Ni$  cluster mainly comes from Zr atom, the partial density of states of Ni and Zr atom for both up and down spins are not symmetrical and the magnetic moment of Ni and Zr atom mainly comes from the electrons of 3d orbital. Both the electronic properties of a typical cluster  $Zr_nNi$  ( $n=2$ ) and the results in Refs. [24] and [25] that the magnetic moment of the clusters  $Zr_2Fe$ ,  $Zr_4Fe$ ,  $ZrCo$  and  $Zr_2Co$  mainly came from Zr atom show our result is credible.

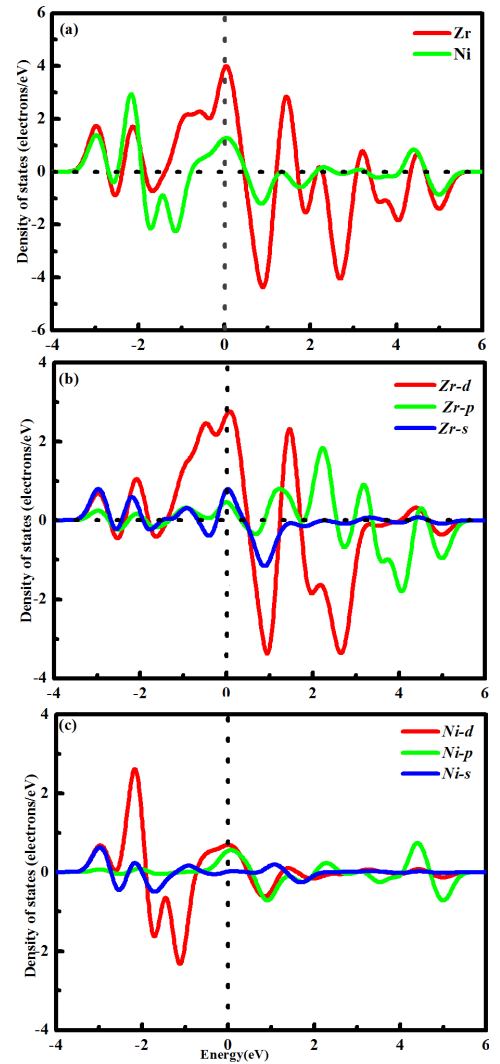


Fig. 5. The total and partial density of states of Zr and Ni atom in  $Zr_2Ni$  cluster ((a),(b) and (c) are total and partial density of states of Zr and Ni atom in  $Zr_2Ni$  cluster).

#### 4. Conclusion

In this paper, the first principles which is based on density functional theory are used to study  $Zr_nNi$  ( $n = 1$  to 9) clusters, the generalized gradient approximation (GGA) is carried out in the optimization and calculation of energy and magnetic features. The results are as follows:

(1)  $Zr_7Ni$  is the most stable of all  $Zr_nNi$  ( $n = 1$  to 9) clusters, who have the largest average binding energies, energy gap and the second-order difference of energy.

(2) The magnetic moment of the ground state  $Zr_nNi$  clusters is about  $4 \mu_B$  for  $n = 1-2$ , however the magnetic moment is about  $2 \mu_B$  for  $n = 2-9$  (except for  $n = 7$ ) from the Muliken population analysis.

(3) Ni atoms get certain charge from Zr atoms and Ni atoms are the electron acceptor for  $Zr_nNi$  clusters.

#### Acknowledgments

This research was supported by the National Natural Science Foundation of China under grant No. 11405280 and the Scientific Research Projects Start-up Foundation of High Level Talented Person of Zhoukou normal college under grant No. ZKNUB2013005.

#### References

- [1] D. Tomanek, S. Mukherjee, K.H. Bennemann, *Phys. Rev. B* **28**, 665 (1983).
- [2] J.J. Zhao, M. Han, G.H. Wang, *Phys. Rev. B* **48**, 15297 (1983).
- [3] Y. Zou, X.M. Tong, J.M. Li, *Acta Phys. Sin.* **44**, 1727 (1995).
- [4] M.D. Morse, *Chem. Rev.* **64**, 4064 (1986).
- [5] Z.Q. Zhao, L.C. Wei, H. Wang, Y.C. Zhong, X.T. Lu, *Acta Phys. Sin.* **46**, 878 (1997).
- [6] C.L. Luo, Z.H. Zhou, *Chin. Phys.* **8**, 820 (1999).
- [7] M.B. Knickelbein, *Ann. Rev. Phys. Chem.* **50**, 79 (1999).
- [8] J.A. Alonso, *Chem. Rev.* **100**, 637 (2000).
- [9] C.L. Luo, Y.H. Zhou, Y. Zhang, *Acta Phys. Sin.* **49**, 54 (2000).
- [10] N.O. Jones, M.R. Beltran, S.N. Khanna, *Phys. Rev. B* **70**, 165406 (2004).
- [11] H.Y. Wang, X.B. Li, Y.J. Tang, H.P. Mao, Z.H. Zhu, *Chin. J. Chem. Phys.* **18**, 50 (2005).
- [12] F. Baletto, R. Ferrando, *Rev. Mod. Phys.* **77**, 371 (2005).
- [13] L. Zhang, C.B. Zhang, Y. Qi, *Chin. Phys.* **16**, 77 (2007).
- [14] Z.H. Zhu, S.Y. Yan, *Chin. Phys.* **15**, 1517 (2006).
- [15] J.J. Zhao, X.S. Chen, Q. Sun, F.Q. Liu, G.H. Wang, K.D. Lian, *Physica B* **215**, 377 (1995).
- [16] G.H. Guo, H.B. Zhang, R.Z. Levitin, *Chin. Phys.* **12**, 655 (2003).
- [17] W.X. Li, B.D. Liu, J.L. Wang, J. Shen, J.H. Wu, F.M. Yang, N.X. Chen, D.B. Frank, *Chin. Phys.* **12**, 661 (2003).
- [18] H.P. Mao, L.R. Yang, H.Y. Wang, Z.H. Zhu, Y.J. Tang, *Acta Phys. Sin.* **54**, 5126 (2005).
- [19] K. Tan, M.H. Lin, N.Q. Wang, Q.E. Zhang, *Acta Chim. Sin.* **63**, 23 (2005).
- [20] P.S. Petko, G.N. Vayssilov, K. Sven, R. Notker, *J. Phys. Chem. A* **111**, 2067 (2007).
- [21] B. Turgut, E. Sakir, H. Masaru, T. Shoichi, *Physica E* **8**, 223 (2000).
- [22] C.C. Wang, R.N. Zhao, J.G. Han, *J. Chem. Phys.* **124**, 194301 (2006).
- [23] W.J. Zhao, X.L. Lei, Y.L. Yan, Z. Yang, Y.H. Luo, *Acta Phys. Sin.* **56**, 5209 (2007).
- [24] W.J. Zhao, Q.L. Wang, F.Z. Ren, Y.H. Luo, *Acta Phys. Sin.* **56**, 5746 (2007).
- [25] F.Z. Ren, Y.X. Wang, F.Y. Tian, W.J. Zhao, Y.H. Luo, *Acta Phys. Sin.* **57**, 2165 (2008).
- [26] F.A. Reuse, S.N. Khanna, S. Bernel, *Phys. Rev. B* **52**, 11650 (1995).
- [27] J. Wang, J.G. Han, *J. Mol. Struct. Theochem.* **718**, 165 (2005).
- [28] J. Wang, J.G. Han, *J. Phys. Chem. B* **110**, 7820 (2006).
- [29] J.G. Yao, X.W. Wang, Y.X. Wang, Q. Jing, Y.H. Luo, *Acta Phys. Sin.* **57**, 4166 (2008).
- [30] Y.D. Dong, G. Gregen, M.G. Scott, *J. Non-Cryst. Solids* **43**, 403 (1982).
- [31] J. Ivkov, E. Babić, *J. Phys. Condens. Matter* **2**, 3891 (1990).
- [32] M.A. Howson, B.L. Gallagher, *Phys. Rep.* **170**, 265 (1988).
- [33] Ž. Marohnić, E. Babić, M. Guberović, G.J. Morgan, *J. Non-Cryst. Solids* **105**, 303 (1988).
- [34] K.N. Lad, A. Pratap, *Physica B* **334**, 135 (2003).
- [35] T. Abe, M. Shimono, M. Ode, H. Onodera, *J. Alloys Comp.* **434-435**, 152 (2007).
- [36] R. Ristić, E. Babić, *J. Non-Cryst. Solids* **353**, 3108 (2007).
- [37] S.H. Wei, Z. Zeng, J.Q. You, X.H. Yan, X.G. Gong, *J. Chem. Phys.* **113**, 11127 (2000).
- [38] J.J. Zhao, Q. Qiu, B.L. Wang, J.L. Wang, G.H. Wang, *Solid State Commun.* **118**, 157 (2001).
- [39] J.J. Zhao, *Phys. Rev. A* **64**, 043204 (2001).
- [40] B. Delly, *J. Chem. Phys.* **92**, 508 (1990).
- [41] S.N. Khanna, B.K. Rao, P. Jena, *Phys. Rev. Lett.* **89**, 016803 (2002).
- [42] J. Wang, J.G. Han, *J. Chem. Phys.* **123**, 064306 (2005).
- [43] X.F. Sheng, G.F. Zhao, L.L. Zhi, *J. Phys. Chem. C* **112**, 17828 (2008).
- [44] S.G. Hao, M.J. Kramer, C.Z. Wang, K.M. Ho, S. Nandi, A. Kreyssig, A.I. Goldman, *Phys. Rev. B* **79**, 104206 (2009).
- [45] M. Brack, *Rev. Mod. Phys.* **65**, 677 (1993).
- [46] W.J. Zhao, Z. Yang, Y.L. Yan, X.L. Lei, G.X. Ge, Q.L. Wang, Y.H. Luo, *Acta Phys. Sin.* **56**, 2596 (2007).